Received: 6 February 2020 | Accepted: 11 February 2020

DOI: 10.1002/maco.202011578

ARTICLE

Materials and Corrosion

Numerical evaluation of the capacity of galvanic anode systems for patch repair of reinforced concrete structures

Christian Helm | **Michael Raupach**

Dedicated to Prof. Dr-Ing. Michael Raupach on the occasion of his 60th birthday

Institute of Building Materials Research, RWTH Aachen University, Aachen, Germany

Correspondence
Christian Helm, Institute of Building Materials Research, RWTH Aachen University, Schinkelstraße 3, 52062 Aachen, Germany.
Email: Helm@ibac.rwth-aachen.de

Funding information
Allianz Industrie Forschung, Grant/Award Number: IGF 20408 N/2

Abstract

Cathodic protection (CP) is an electrochemical repair or corrosion prevention technique for steel structures exposed to a corrosive environment. For reinforced concrete (RC) usually impressed current CP is used, due to the comparably high resistivity of the concrete, serving as electrolyte. Nevertheless, the market provides a wide range of galvanic anode systems for RC structures. Their most common use is the application within the framework of partial concrete replacement due to chloride-induced corrosion. This patch repair is often accompanied by the so-called anode ring effect, causing accelerated corrosion of the rebar in the substrate concrete in the vicinity of repair patches. This is caused by the cathodic capabilities of the repassivated rebar. Galvanic anodes are reported to prevent this effect. In this paper, a numerical model is proposed, which is capable of determining the effectiveness of the method dependent on, for example, the type and quantity of anodes, rebar content, and geometry or climatic conditions. The method is presented for a specific set of input parameters and the applicability is discussed against the background of different protection criteria.

KEYWORDS

cathodic protection, galvanic anodes, numerical modeling, reinforced concrete

1 | INTRODUCTION

The use of galvanic anodes is the initial form of cathodic protection (CP). It is still used in a wide range of applications, such as CP of pipelines, ships or offshore steel structures. For CP of reinforced concrete (RC) structures, impressed cathodic protection (ICCP) has prevailed. Nevertheless, galvanic anodes can provide simple and cost-effective corrosion protection for several RC applications, see References[1–7] for example. A common field of application is the use within the framework of partial concrete replacement to prevent the so-called anode ring effect. The cost-effectiveness of the method results from the simple installation and the absence of controlling devices. However, this absence prevents any verification of the effectiveness and durability of the measure. Hence, the use of this method is limited due to uncertainty and liability issues. Therefore, a joint research project of the Institute for Building Materials Research, RWTH-Aachen University, Germany, (ibac) and the Federal Institute for Materials Research and Testing, Berlin, Germany (BAM), has been set up to determine the performance of these

systems and their temporal development. In this project, the polarization behavior of galvanic anodes from numerous manufacturers is determined as a function of time. To transfer the results to practical conditions, numerical methods are applied. The numerical approach developed in the scope of this project is presented below.

2 | THEORETICAL BACKGROUND

2.1 | Corrosion of steel in concrete

Steel in concrete is protected against corrosion due to the highly alkaline pore solution that leads to the formation of a dense passive layer on the steel surface. This layer prevents the anodic dissolution of iron. To initiate corrosion, a breakdown of this passive layer is necessary. This can either be caused by the loss of alkalinity because of carbonation or by the ingress of chlorides. In this study, only chloride-induced corrosion is discussed as a possible field of application. The chlorides usually penetrate the concrete cover from the surface (e.g., de-icing salts, seawater in the marine environment). It is characterized by a pitting kind of corrosion, where anodic and cathodic areas are spatially separated. This can cause a rapid loss of cross-section and high corrosion rates because of a high cathode-to-anode area ratio. The driving force of the corrosion process is the potential difference between the anode and cathode, in this case, formed by the actively corroding rebar and the rebar that still remains passive. Between these areas, a so-called macrocell is formed.

2.2 | CP of steel in concrete

CP is an electrochemical repair method for RC structures affected by chloride-induced corrosion. It is based on a cathodic polarization of the corroding rebar to potentials below the corrosion potential of the macrocell. This directly impedes the anodic dissolution of iron. Furthermore, the potential differences between anodic and cathodic areas are leveled, which reduces the level of macrocell activity. Early CP applications on RC structures were realized by use of galvanic anode systems, for example, discrete, sprayed, or adhesive zinc anodes.[1,8] Nowadays, mainly ICCP is used, where the protection current is provided to the structure via mixed metal oxide -coated titanium anodes by use of a rectifier. Although the driving voltage in these cases is adjustable, it is predetermined by the potential difference between anode material and corrosion potential of the rebar in the case of galvanic CP. This results in maximum driving voltages of a few 100 mV for commonly used zinc-based anodes. Therefore, these anodes cannot be expected to fulfill the common protection criteria for CP[9] for a wide range of applications due to the relatively high resistivity of the concrete. Except for some successful installations in tidal zones of marine structures, the main application of these anodes is in the framework of partial concrete replacement to prevent the so-called anode ring effect.

2.3 | The anode ring effect

Chloride-induced corrosion of reinforced concrete usually causes spatially separated anodic and cathodic areas. For slab -like structures, such as parking decks, these spots can be located next to each other on the top side, from where the chloride ingress also originates. Here, the cathodic areas may also exceed the critical chloride threshold level, but due to cathodic protection by the stronger macrocell anode nearby, active corrosion is prevented. As soon as this anode is refurbished by replacement of the contaminated concrete with repair mortar, the protective cathodic polarization is replaced by an anodic polarization caused by the repassivated rebar in the repair mortar. Corrosion initiation accelerated corrosion and subsequent cracking and spalling around the repair patch may result, (see References[3,6,10] for example).

The simple installation of galvanic anodes and the complete absence of any active control system are the major benefits of this method. Thus, the effectiveness of a repair measure can only be assessed phenomenologically. In this study, numerical methods are applied, to allow for general considerations.

2.4 | Numerical modeling of RC corrosion and CP

Any arrangement of electrically connected anodes and cathodes inside an electrolyte will result in the formation of certain potentials on the electrode surfaces. This causes the formation of a spatially variable electrical field inside the electrolyte. The resulting current densities of the anodic and cathodic reactions can then be assessed by use of the following boundary conditions[11]:

The potential distribution inside the concrete can be described by Laplace's Equation (1), assuming that the electrolyte is homogeneous:

$$\nabla^2 E = 0. \tag{1}$$

The current flow in any direction results in:

$$I_{xj} = \sigma \cdot \nabla E. \tag{2}$$

The total current density for any part of the electrode surfaces can be calculated via Ohm's law:

$$I_s = \sigma \cdot \frac{\partial E}{\partial n}, \tag{3}$$

where E is the potential, ∇^2 is the Laplace operator, I_{xj} is the current flow in direction xj, and I_s is the total current density, with

$$\sigma = \frac{1}{\rho}, \tag{4}$$

where ρ is the resistivity.

The vector normal to the potential gradient has to be zero at all isolating surfaces:

$$\frac{\partial E}{\partial n} = 0. \tag{5}$$

Due to electroneutrality the sum of all currents inside the system has to be zero as well:

$$\int_F i dA = \int_{F_a} i_a dA + \int_{F_c} i_c dA = 0. \tag{6}$$

The current density is a function of the electrode potential and can be described by a polarization curve for each electrode:

$$i_a = f_a(E_a), \tag{7}$$

$$i_c = f_c(E_c), \tag{8}$$

where i_a is the current density of the anodic reaction, i_c is the current density of the cathodic reaction, E_a is the anodic potential, E_c is the cathodic potential, f_a is the anodic polarization curve, and f_c is the cathodic polarization curve.

The equations above allow an analytical calculation of Laplace's equation for any given set of linear polarization curves. In the case of nonlinear polarization behavior, numerical methods have to be applied.

A common method to assess the respective polarization properties expressed by Equation (7) and (8) is the realization of potentiodynamic experiments, see Section 3. The implementation in the numerical calculations is usually achieved by fitting the results with the Butler–Volmer equation:

$$i = \frac{i_0 \cdot \left[\exp\left(\frac{2.3 \cdot \eta}{b_a}\right) - \exp\left(\frac{-2.3 \cdot \eta}{b_c}\right)\right]}{1 + \frac{i_0}{i_{lim,ox}} \cdot \exp\left(\frac{2.3 \cdot \eta}{b_a}\right) - \frac{i_0}{i_{lim,red}} \cdot \exp\left(\frac{-2.3 \cdot \eta}{b_c}\right)}, \tag{9}$$

where i is the current density on the steel surface, i_0 is the exchange current density, η is the overpotential $(E - E_0)$, E is the potential, E_0 is the free corrosion potential, b_a is the anodic Tafel slope, b_c is the cathodic Tafel slope, $i_{lim,ox}$ is the limiting current density of the anodic reaction, and $i_{lim,red}$ is the limiting current density of the cathodic reaction.

For modeling CP of RC structures, the CP anode system has to be added. Although several different methods exist to represent ICCP anode systems,[12] galvanic anodes can be treated using the same methods presented above. The cathodic polarization of the rebar is then achieved by use of CP anode materials, which provide more negative free corrosion potentials in the alkaline environment than the active rebar. The protection current density, in this case, can also be described as a function of the potential:

$$i_{cpa} = f_{cpa}(E_{cpa}), \tag{10}$$

where i_{cpa} is the current density of the CP anode and E_{cpa} is the CP anode potential.

Hence, numerical modeling of galvanic CP does not require any systematic changes in the modeling process except the addition of the CP anode system. As the protection current is created by active corrosion of the CP anode, the service life is limited either by complete consumption of the anode material, the formation of nonconductive oxide layers in the anode concrete interface or bond loss.

3 | EXPERIMENTAL

3.1 | Determination of input parameters

3.1.1 | Resistivity

For the numerical study presented below, a realistic set of combinations of the resistivity of substrate concrete and repair mortar for on-site conditions was needed. Thus, in the first step, water content to resistivity relations was determined.

For this purpose, cores with a diameter of 100 mm were drilled from the concrete as well as from the repair mortar. The concrete was based on ordinary Portland cement and designed for exposure class XD3.[13] The repair mortar used in this study was a randomly chosen, commercially available product, often used for concrete replacement.

These cores were cut to slices with a thickness of approximately 15 mm. The concrete surfaces in contact with the air or the mold were abandoned. The slices were ponded in tap water at atmospheric conditions until their mass was considered to be constant. Afterward, the resistance of each slice was determined by means of the

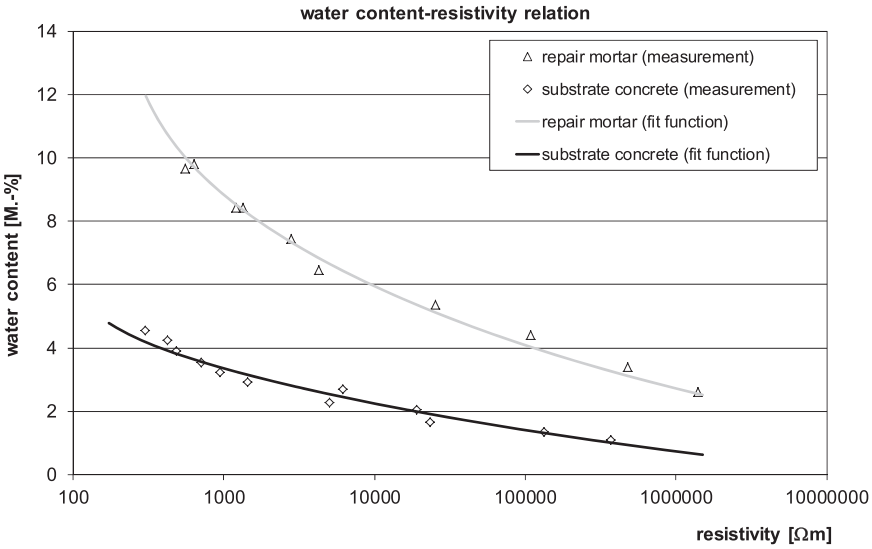

FIGURE 1 Water content-resistivity relations of substrate concrete and repair mortar For both materials, fit functions were calculated, using Equation (12), according to References[14,15]

two-electrode method, using alternating current at a frequency of 1,000 Hz. The specimens were weighed directly after the resistivity measurement. Then, they were stored in a drying chamber at 70°C until the mass loss was lower than 0.1 g per week. Then again, water was added in increasing steps, to cover the range of water contents from dry to water-saturated. The specimens were then vacuumed and stored in vapor-proof packing for more than 6 weeks, to allow the water to distribute homogeneously. At the end of this period, the specimens were taken out of the packing and the resistance and related mass were reassessed. Finally, all specimens were dried until mass constancy at 105°C. From these data, the resistivity of each slice at two different moisture conditions was calculated using the real dimensions of each specimen (see the following equation):

$$k_e = \frac{l}{A}, \tag{11}$$

where k_e is the cell constant of macrocell, l is the distance between the parallel electrodes, and A is the electrode surface.

The resulting values are presented in Figure 1.

$$u = \frac{A}{\ln(B \cdot \rho + C) - D} + E, \tag{12}$$

where u is the water content in % per weight, ρ is the resistivity, and A–E are the regression parameters.

The related parameters are given in Table 1.

In this study, the fit function is only used as a means of interpolation within the range of observed values. It does not claim to provide any theoretical background allowing for extrapolation.

3.1.2 | Sorption

Although the resistivity for different water contents is known now, additional information is needed to determine sets of input parameters. Mortar and concrete will acquire different water contents, stored at the same relative humidity (RH). Therefore, additional specimens were cut from the slices mentioned above in the water-saturated state and then stored in different desiccators for several months until equilibrium. Subsequently, the water contents were determined by drying at 105°C. The results are presented in Figure 2. Again, fit functions allowing for interpolation in the observed range of values were calculated. The fit function is given in the below equation. The parameters are presented in Table 2.

$$u = A + B \times \mathrm{RH}^C, \tag{13}$$

TABLE 1 Regression parameters for the fit functions of the water content-resistivity relation of concrete and repair mortar

Material	*A* (M.-%)	*B* (1/Ωm)	*C*	*D*	*E* (M.-%)
Repair mortar	159.396	47.900	−7,887.798	0.092	−6.339
Concrete	144.848	89.530	−7,256.569	−5.155	−5.438

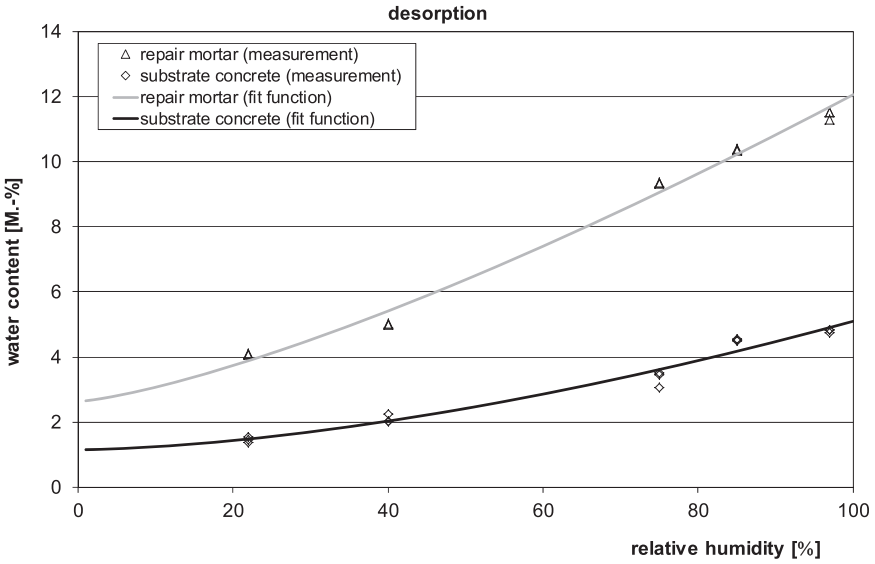

FIGURE 2 Desorption characteristics of substrate concrete and repair mortar

TABLE 2 Regression parameters for the fit functions for the desorption behavior of concrete and repair mortar

Material	*A* (M.-%)	*B* (M.-%)	*C*
Repair mortar	2.63614	0.02030	1.3333
Concrete	1.1536	0.00208	1.63896

where u is the water content in % per weight, RH is the relative humidity, and A–C are the regression parameters.

3.1.3 | Polarization properties

To allow for a realistic calculation of current and potential distribution, the polarization behavior of active and passive reinforcement, as well as galvanic anode, has to be assessed in the form of current density curves. Figure 3 presents a schematic visualization of the used test setup and specimen layout. To determine the anode surface area as well as the mass of the zinc, an autopsy was conducted on one of the anodes. Figure 4 shows the galvanic anode used in this study before and after removal of the embedding mortar. The polarization testing was done by potentiodynamic polarization with a feed rate of 2 mV/min. The ohmic drop was removed from the readings by means of instant-off measurements and linear compensation. The result is given in Figure 5. The polarization properties of the active and passive rebar have been determined in previous studies[16,17] and have already been used for modeling of CP.[17,18] They represent the polarization behavior of the rebar before permanent cathodic protection. Long term application of CP may change these properties.[16–18] The related fit

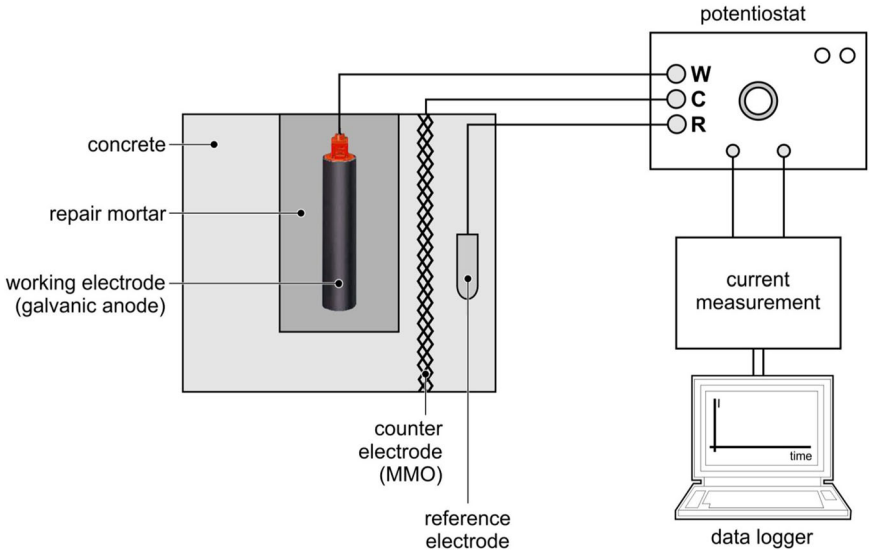

FIGURE 3 Setup for polarization experiment [Color figure can be viewed at wileyonlinelibrary.com]

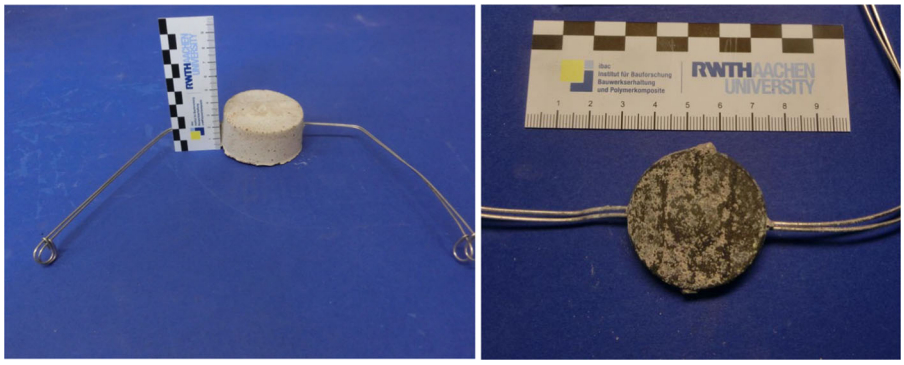

FIGURE 4 Galvanic anode (left) and embedded zinc disc after autopsy (right) [Color figure can be viewed at wileyonlinelibrary.com]

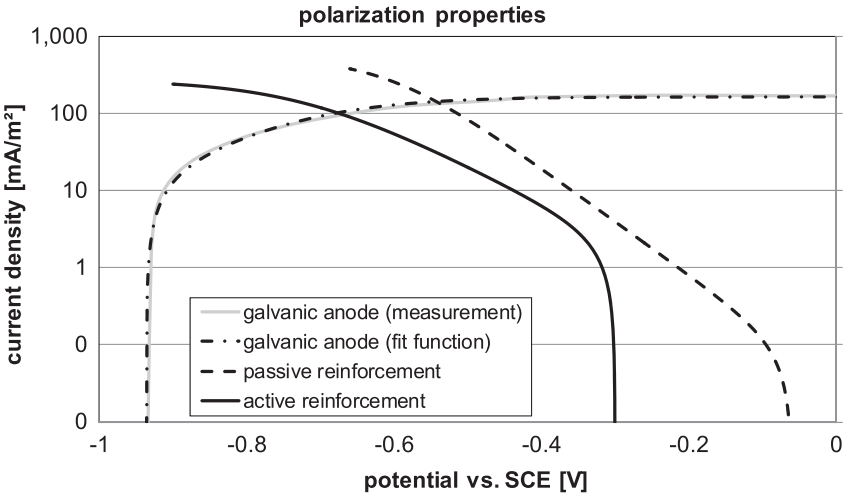

FIGURE 5 Polarization properties of galvanic anode and reinforcement. SCE, saturated calomel electrode

parameters for Equation (9) are given in Table 3. These parameters have been chosen to approximate the measured curves. However, some of the parameters may not be within the range of their theoretical limits. This can be caused, for example, by transport limitations, oxide layers, or downstream reactions.

3.2 | Geometry

For this study, a slab-like geometry with a centric repair patch has been chosen. The diameter of the patch was set to 1 m. To use symmetry, only a quarter of the slab was modeled (see Figure 6). The dimensions of the model geometry are 1.5 by 1.5 m^2 with a thickness of 0.2 m and a concrete cover of 35 mm at the top and bottom sides. Two layers of reinforcing steel mesh with a diameter of 6 mm and lateral spacing of 0.15 m were chosen as rebar. For simplification, the rectangular rods were assumed to be in the same depth layer, reducing the number of elements at the crossings significantly. The repair patch has a diameter of 0.5 m and a depth of 47 mm. This means that the rebar within the repair match is enclosed in the repair mortar completely. The galvanic anodes have a diameter of 38 mm and a thickness of 8.4 mm, as determined by autopsy (see Figure 4). The center is located on a circular path with a 50-mm distance to the edge of the patch. The vertical distance to the rebar is set to 10.8 mm, which is the actual thickness of the anode embedding mortar.

TABLE 3 Fit parameters for the polarization properties used within this study

Electrode	E_0 (V)	i_0 (A/m²)	b_a (V/dec)	b_c (V/dec)	$i_{lim,ox}$ (A/m²)	$i_{lim,red}$ (A/m²)
Passive rebar	−0.06	0.0000858	0.15	0.1438	1	0.545
Active rebar	−0.3	0.002234	0.15	0.202	1	0.273
Galvanic anode	−0.936	0.018	0.22	0.18	0.165	1.2

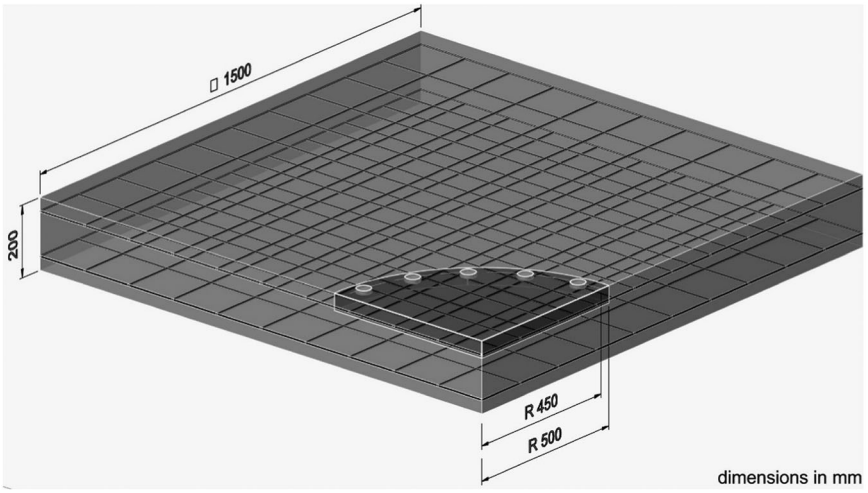

FIGURE 6 Model geometry (example for 20 pcs of galvanic anodes)

3.3 | Parametric study

In the numerical study presented below, the number of galvanic anodes, as well as different concrete and mortar resistivities, were varied. As the model geometry does not provide real point symmetry due to the rectangular arrangement of the rebar, the number of anodes was varied in steps of one additional anode per quadrant, equivalent to four additional anodes in the whole repair spot. The anodes were distributed centered and equidistantly on their circular path, causing the rebar on the symmetry edges of the model to have the maximum distance to an anode for each step. Three sets of concrete resistivity were chosen for the study. The combinations were picked using the relationships determined in Sections 3.1.1 and 3.1.2. For the dry case, a medium RH of 75% was chosen as a lower limit for roofed outside storage in Germany. To determine the impact of more humid climates, 85% and 95% RH were investigated additionally. For each humidity, the related water contents of mortar and concrete were derived from the fit functions given in Figure 2 and Equation (13) using the parameters given in Table 2. The resulting resistivities were calculated analogously, using Equation (12) and Table 3. The parameters used for the study are given in Table 4. A divergent resistivity of the embedding mortar of the galvanic anode was neglected in this study. The lower reinforcement layer, as well as the rebar enclosed in the repair mortar, was defined as passive, while the complete upper reinforcement in the substrate concrete was defined to be in an active corrosion state, using the polarization properties discussed above. The calculations were conducted using the software COMSOL Multiphysics 5.3a.

4 | RESULTS AND DISCUSSION

To analyze the effectiveness of the different amounts of galvanic anodes for the investigated climatic conditions, the current and potential distribution of the upper reinforcing bar along the symmetry axis, represented by the edge of the geometry given in Figure 6, was investigated. This is assumed to be on the safe side, as the distance to the galvanic anode is maximized for each step. Furthermore, the rebar surface in this section is maximized too. Figure 7 presents the potential distribution on the ridge of the bar under investigation for permanent storage at 75% RH. The boundary of the repair patch and the substrate concrete is at 0.5 m, visualized by the vertical line. The top graph represents the free corrosion occurring in the slab without the installation of any galvanic anode in the repair patch. The other graphs show the impact of a rising number of equidistant galvanic anodes within the patch. The distance between the anodes is given in the legend. Although four anodes mean that only one galvanic anode is installed per

TABLE 4 Input parameters for concrete and mortar resistivity

Relative humidity (%)	Water content mortar (M.-%)	Resistivity mortar (Ωm)	Water content concrete (M.-%)	Resistivity concrete (Ωm)	Ratio
75	9.06	880	3.62	649	1.36:1
85	10.22	512	4.18	305	1.68:1
95	11.43	345	4.78	173	1.99:1

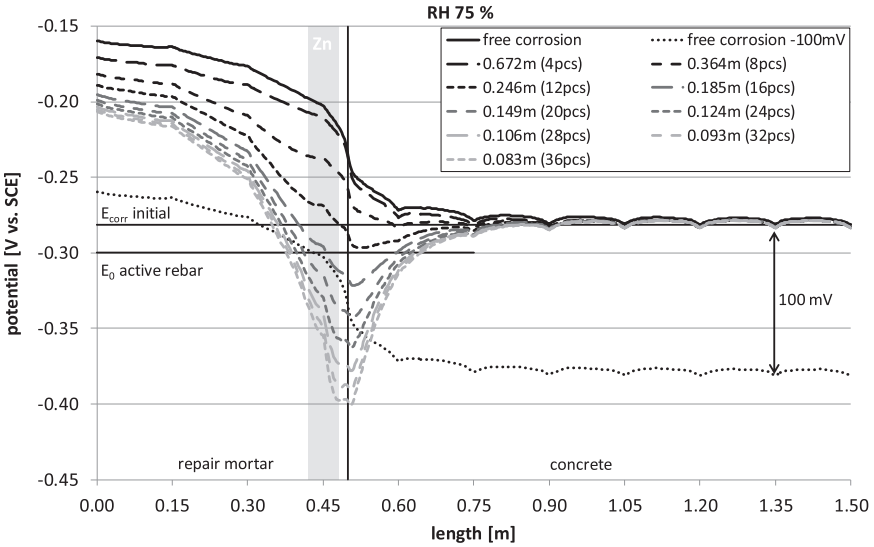

FIGURE 7 Potential distribution along the symmetry axis for different quantities of galvanic anodes; calculated for relative humidity (RH) of 75%. SCE, saturated calomel electrode

quadrant, the number of 36 anodes represents a theoretical maximum, as the spacing of 83 mm is close to the diameter of the anode, which is approximately 60 mm including the embedding mortar. It is evident that in the part further away from the patch, the potential distribution is independent of the number of anodes. The corrosion activity is dominated by the macro element between the top and bottom rebar. The free corrosion graph shows that the active rebar is polarized to more anodic values in the area between 0.5 and 1 m. This means, that the throwing power of the new cathode formed by the repassivated rebar is about 0.3 m for this set of input parameters. It is also a numerical proof of the anode ring effect. Obviously, any number of galvanic anodes is capable of reducing the magnitude and the extent of the effect. Amounts of more than 12 anodes reduce polarization below the value $E_{\text{corr; initial}}$, caused by the macro element between the top and bottom rebar in the unrepaired part (see Figure 7). This means that the existence of the repair patch is now masked for the active rebar. This can be regarded as the first level of corrosion protection for galvanic anodes. Higher amounts are capable of reducing the polarization below the free corrosion potential of the rebar, $E_{0\ \text{active rebar}}$ (see Figure 7). In this case, the net corrosion currents are cathodic and the macro element is suppressed for the bottom rebar too. This could be defined as the second level of protection. The effect is locally limited and the distance where it is covered is rising with the amount of galvanic anodes. It can be also visualized by evaluating the current distribution on the rebar surface (see Figure 8). The point of discontinuity in the graphs represents the boundary of repair mortar and concrete. As the current distribution is linked to the

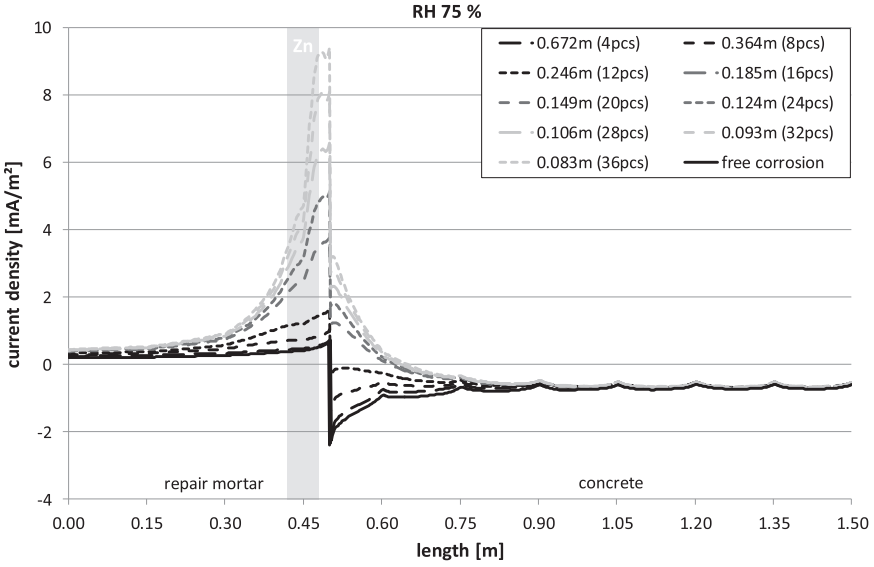

FIGURE 8 Current density distribution along the symmetry axis for different quantities of galvanic anodes, calculated for relative humidity (RH) of 75%

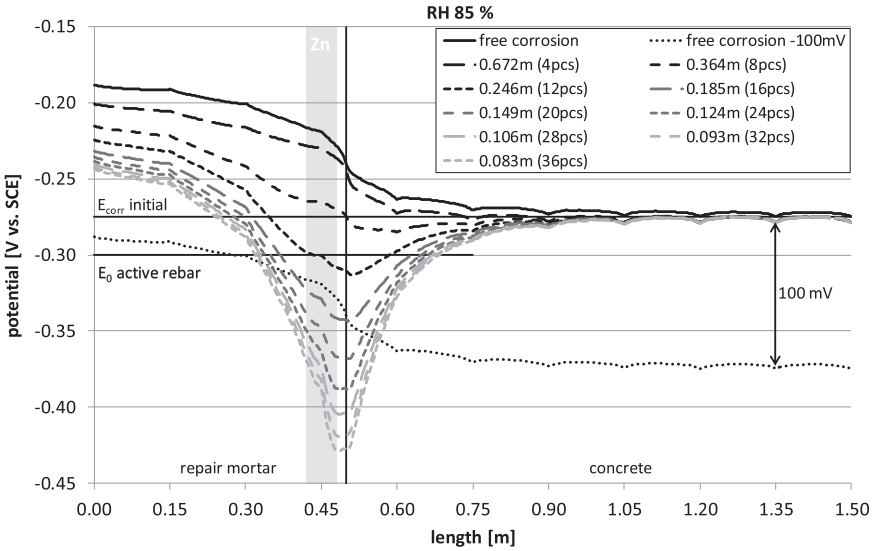

FIGURE 9 Potential distribution along the symmetry axis for different quantities of galvanic anodes, calculated for relative humidity (RH) of 85%. SCE, saturated calomel electrode

potential distribution by the current density curves presented in Section 3 (see Figure 5), the effect of increasing amounts of anodes is also evident, leading to more cathodic currents, defined as positive. Within this visualization, the extent of the macro element suppression is defined by the point of intersection of the respective graph with the zero axis. For the parameters investigated so far, the range of this effect seems to be more or less independent of further increase in the amount of anodes, once the macro element is suppressed. The third level of corrosion protection could be the compliance with the 100-mV decay criterion,[9] meaning that the galvanic anodes are capable of similar performance as an ICCP system for the given boundary conditions. Whether this is feasible or not can also be discussed on the basis of Figure 7. The dotted line labeled −100 mV is the potential distribution of the free corrosion case, shifted by 100 mV in the negative direction. Although other definitions exist, the shortfall of this value can be interpreted as local compliance with the criterion, which is in practice dependent on the positioning of the reference electrode within the concrete domain. This topic is discussed in Reference[18] extensively. Using the definition above, it becomes obvious that compliance with this criterion can only be achieved in a small area around the boundary between patch and concrete, using high amounts of galvanic anodes.

The observations above apply for rather dry conditions. Figures 9–12 show the results for 85% and 95% RH respectively. The general observation is that the magnitude of polarization and corrosion currents increases with higher RH. The same applies to the throwing power of the passive reinforcement within the repair

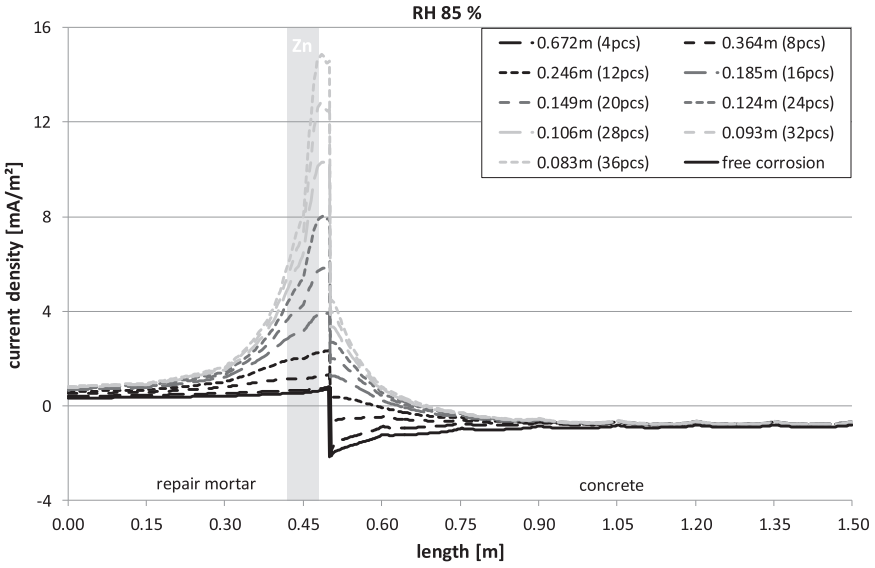

FIGURE 10 Current density distribution along the symmetry axis for different quantities of galvanic anodes, calculated for relative humidity (RH) of 85%

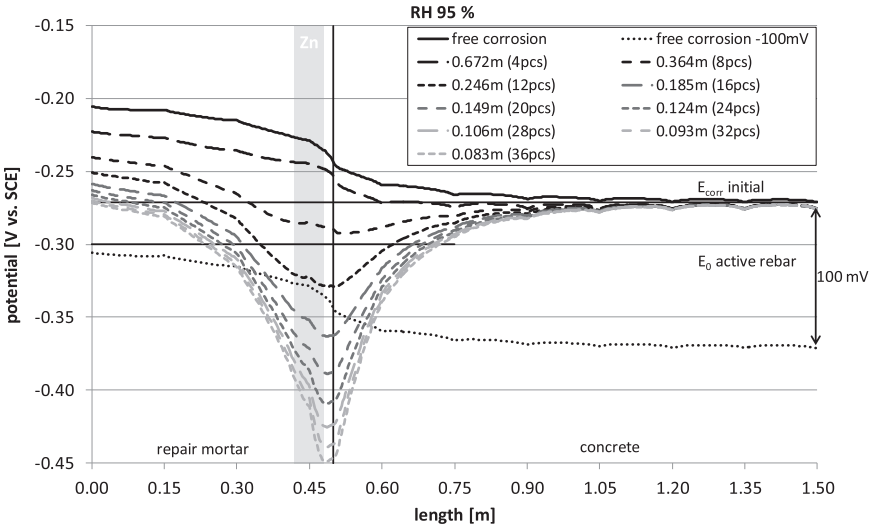

FIGURE 11 Potential distribution along the symmetry axis for different quantities of galvanic anodes, calculated for relative humidity (RH) of 95%. SCE, saturated calomel electrode

mortar and the galvanic anodes. This is expectable for a lower concrete resistivity. The main question to be answered by interpreting these results is whether the lower resistivity is beneficial to the effectiveness of the galvanic anodes or if this effect is overcompensated by the macrocell activity within the slab, which is also promoted. To answer this question, all results have been investigated regarding their compliance with the three levels of protection discussed above and its extent. The results are summarized in Table 5. It is evident that the number of anodes needed to achieve the different levels of protection discussed above is generally decreasing with higher RH. Coverage of all levels is possible with amounts from 12 (wet) to 20 (dry) pieces of anodes per patch, corresponding to anode spacing from approximately 250 to 150 mm along the edge of the repair patch. Higher amounts of anodes increase the distance of coverage only in a very limited range for the chosen geometry. To judge whether more anodes per patch provide a longer theoretical service life, the mean anode current densities on the surface of the galvanic anodes were calculated from the modeling data. From these, the maximized service life has been calculated by use of Faraday's law, assuming a mass of 60 g zinc per anode, as assessed via autopsy. The results are also presented in Table 5. It can be seen that the anode current densities can only be reduced insignificantly by use of further anodes. This is probably caused by the high cathodic capabilities of the chosen geometry and rebar distribution. This may lead to an anodic control of the corrosion system. The resulting service life calculations show unrealistic high results. The actual service life may be significantly shorter due to the formation of oxide layers, pore-blocking effects, or the loss of electrolytic contact at the anode to mortar interface. This will be further investigated within the course of the project.

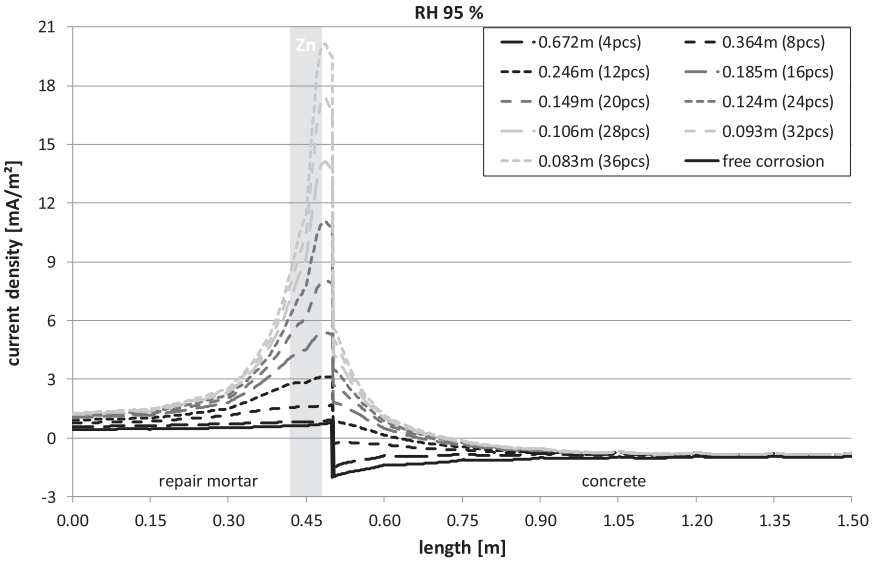

FIGURE 12 Current density distribution along the symmetry axis for different quantities of galvanic anodes, calculated for relative humidity (RH) of 95%

TABLE 5 Summary of results

RH (%)	Anodes for masking patch (-)	Distance for macrocell suppression (m)	Distance for 100 mV decay (m)	Mean current density on anode surface (mA/m^2)	Theoretical service life[b]
75	12	–[a]	–[a]	2.57	62
	16	0.098	–[a]	2.32	69
	20	0.112	0.004	2.22	72
	24	0.125	0.024	2.27	70
	28	0.136	0.034	2.10	76
	32	0.140	0.041	2.04	78
	36	0.145	0.044	1.88	85
85	8	–[a]	–[a]	4.78	33
	12	0.087	–[a]	4.44	36
	16	0.129	0.004	3.99	40
	20	0.149	0.034	3.79	42
	24	0.162	0.047	3.82	42
	28	0.171	0.058	3.53	45
	32	0.179	0.062	3.40	47
	36	0.184	0.065	3.13	51
95	8	–[a]	–[a]	6.95	23
	12	0.125	0.000	6.43	25
	16	0.166	0.030	5.79	28
	20	0.184	0.047	5.48	29
	24	0.197	0.065	5.45	29
	28	0.210	0.072	5.03	32
	32	0.214	0.078	4.81	33
	36	0.221	0.081	4.44	36

[a]Not fulfilled for given number of anodes.
[b]Assuming that the total amount of zinc is consumed to protection current.

5 | CONCLUSIONS

In this study, the capabilities of a commercially available galvanic anode in the framework of partial concrete replacement have been assessed by means of numerical studies. From the results, the following conclusions can be drawn:

- Galvanic anodes are capable of inhibiting the so-called anode ring effect often observed when using partial concrete replacement
- The electrochemical masking of the new cathode area within the repair mortar, local suppression of macro-elements or even the local compliance with the 100-mV decay criterion can be achieved for realistic climate conditions and reasonable anode spacings
- The throwing power is limited, the effect is evident in a rather small area around the boundary of repair mortar and substrate concrete only
- Even anode spacings of approximately 250 mm near the concrete-mortar interface allow for an effective electrochemical decoupling of the new cathode in the repair patch in case of severe corrosion, such as the complete depassivation of the upper rebar layer

6 | OUTLOOK

Within the scope of the ongoing research project, the investigations presented above will be repeated using six other types of commercially available galvanic anode systems to analyze the impact of different geometries or activation mechanisms. Furthermore, the polarization properties will be assessed as a function of time and emitted charge, to allow for time-dependent assessment of the performance and realistic service life prognosis. Geometrical parameters like the distance between upper and lower rebar layer, rebar content, and especially, the

distribution of active and passive rebar areas should be further investigated, as they seem to have a significant impact on the effectiveness of the method. Furthermore, the interactions between galvanic anodes and surface applied coating systems should be investigated.

ACKNOWLEDGMENTS

The authors would like to thank the German Federation of Industrial Research Association (AiF) for the funding of this study. This study was funded by the AiF e. V. within the IGF program on behalf of the German Federal Ministry for Economic Affairs and Energy (project 20408N of the GfKORR e. V.).

ORCID

Christian Helm http://orcid.org/0000-0002-2995-5260

REFERENCES

[1] M. Raupach, presented at Technische Forschung und Beratung für Zement und Beton, TFB. Fachveranstaltung 824761/62, Betoninstandsetzung—aus Fehlern lernen, Wildegg, Switzerland, February and May, **2003**.
[2] O. Troconis de Rincon, Y. Hernandez-Lopez, A. Valle-Moreno de, A. A. Torres-Acosta, F. Barrios, P. Montero, P. Oidor-Salinas, J. Rodriguez-Montero, *Constr. Build. Mater.* **2008**, *22*, 494.
[3] C. Christodoulou, J. Webb, G. Glass, S. Austin, C. Goodier *Proc. 4th Int. Conf. Concr. Repair, 2011* (Eds: M. Grantham, V. Mechtcherine, U. Schneck), CRC Press, London, UK **2011**.
[4] V. Rajendran, R. Murugesan, *ARPN J. Eng. Appl. Sci.* **2011**, *6*, 45.
[5] S. P. Holmes, G. D. Wilcox, P. J. Robins, G. K. Glass, A. C. Roberts, *Corros. Sci.* **2011**, *53*, 3450.
[6] G. Sergi, *Mater. Corros.* **2011**, *62*, 98.
[7] G. Glass, C. Christodoulou, S. P. Holmes, in *Proc. 3rd Int. Conf. Concr. Repair Rehabilitat. Retrofit., ICCRRR* (Ed: M. G. Alexander), London: Taylor & Francis Group; **2012**, pp. 523–526.
[8] M. Raupach, M. Bruns, presented at 15th Int. Corros. Congr., Front. Corros. Sci. Technol., Granada, Spain, September, **2002**.
[9] DIN EN ISO 12696:2012–05, Cathodic protection of steel in concrete, **2012**
[10] M. Raupach, *Cem. Concr. Compos.* **2006**, *28*, 679.
[11] M. Brem, *Ph.D. Thesis*, Eidgenössische Technische Hochschule (Zürich, Switzerland) **2004**.
[12] C. Helm, M. Raupach, *Mater. Corros.* **2016**, *67*, 621.
[13] DIN EN 206:2017-06, Concrete—Specification, performance, production and conformity, **2016**
[14] J. Harnisch, *Ph.D. Thesis*, RWTH Aachen, Aachen, Germany **2003**.
[15] W. Brameshuber, M. Raupach, P. Schröder, C. Dauberschmidt, presented at Int. Symp. Non-Destruct. Test. Civil Eng. (NDT-CE), Berlin, Germany, September, **2003**.
[16] T. Eichler, *Ph.D. Thesis*, RWTH-Aachen University, Aachen, Germany **2012**.
[17] C. Helm, T. Eichler, M. Raupach, B. Isecke, presented at EUROCORR 2011, Stockholm, Sweden, September **2011**.
[18] C. Helm, M. Raupach, *Mater. Corros.* **2019**, *70*, 642.

How to cite this article: Helm C, Raupach M. Numerical evaluation of the capacity of galvanic anode systems for patch repair of reinforced concrete structures. *Materials and Corrosion*. 2020;1–12. https://doi.org/10.1002/maco.202011578